Binding H_2, N_2, H^-, and BH_3 to Transition-Metal Sulfur Sites: Synthesis and Properties of [Ru(L)(PR_3)($N_2Me_2S_2$)] Complexes (L = η^2-H_2, H^-, BH_3; R = Cy, *i*Pr)**

D. Sellmann,†[a] A. Hille,*[a] F. W. Heinemann,[a] M. Moll,[a] M. Reiher,[b] B. A. Hess,[b] and W. Bauer[c]

Abstract: The reactions of [Ru(N_2)(PR_3)('$N_2Me_2S_2$')] ['$N_2Me_2S_2$' = 1,2-ethanediamine-*N*,*N*′-dimethyl-*N*,*N*′-bis(2-benzenethiolate)(2−)] [**1a** (R = *i*Pr), **1b** (R = Cy)] and [μ-N_2{Ru(N_2)($PiPr_3$)('$N_2Me_2S_2$')}$_2$] (**1c**) with H_2, $NaBH_4$, and NBu_4BH_4, intended to reduce the N_2 ligands, led to substitution of N_2 and formation of the new complexes [Ru(H_2)(PR_3)('$N_2Me_2S_2$')] [**2a** (R = *i*Pr), **2b** (R = Cy)], [Ru(BH_3)(PR_3)('$N_2Me_2S_2$')] [**3a** (R = *i*Pr), **3b** (R = Cy)], and [Ru(H)(PR_3)('$N_2Me_2S_2$')]$^-$ [**4a** (R = *i*Pr), **4b** (R = Cy)]. The BH_3 and hydride complexes **3a**, **3b**, **4a**, and **4b** were obtained subsequently by rational synthesis from **1a** or **1b** and BH_3·THF or $LiBEt_3H$. The primary step in all reactions probably is the dissociation of N_2 from the N_2 complexes to give coordinatively unsaturated [Ru(PR_3)('$N_2Me_2S_2$')] fragments that add H_2, BH_4^-, BH_3, or H^-. All complexes were completely characterized by elemental analysis and common spectroscopic methods. The molecular structures of [Ru(H_2)(PR_3)('$N_2Me_2S_2$')] [**2a** (R = *i*Pr), **2b** (R = Cy)], [Ru(BH_3)($PiPr_3$)('$N_2Me_2S_2$')] (**3a**), [Li(THF)$_2$][Ru(H)($PiPr_3$)('$N_2Me_2S_2$')] ([Li(THF)$_2$]-**4a**), and NBu_4[Ru(H)(PCy_3)('$N_2Me_2S_2$')] (NBu_4-**4b**) were determined by X-ray crystal structure analysis. Measurements of the NMR relaxation time T_1 corroborated the η^2 bonding mode of the H_2 ligands in **2a** (T_1 = 35 ms) and **2b** (T_1 = 21 ms). The H,D coupling constants of the analogous HD complexes HD-**2a** (^1J(H,D) = 26.0 Hz) and HD-**2b** (^1J(H,D) = 25.9 Hz) enabled calculation of the H−D distances, which agreed with the values found by X-ray crystal structure analysis (**2a**: 92 pm (X-ray) versus 98 pm (calculated), **2b**: 99 versus 98 pm). The BH_3 entities in **3a** and **3b** bind to one thiolate donor of the [Ru(PR_3)('$N_2Me_2S_2$')] fragment and through a B-H-Ru bond to the Ru center. The hydride complex anions **4a** and **4b** are extremely Brønsted basic and are instantanously protonated to give the η^2-H_2 complexes **2a** and **2b**.

Keywords: dihydrogen ligands · hydride ligands · N ligands · ruthenium · S ligands

[a] Prof. Dr. D. Sellmann,† Dr. A. Hille, Dr. F. W. Heinemann, Dr. M. Moll
Institut für Anorganische Chemie
der Universität Erlangen-Nürnberg
Egerlandstrasse 1, 91058 Erlangen (Germany)
Fax: (+49) 9131857367
E-mail: hille@anorganik.chemie.uni-erlangen.de

[b] Priv.-Doz. Dr. M. Reiher, Prof. Dr. B. A. Hess
Institut für Theoretische Chemie
der Universität Bonn
Wegelerstrasse 12, 53115 Bonn (Germany)

[c] Prof. Dr. W. Bauer
Institut für Organische Chemie
der Universität Erlangen-Nürnberg
Henkestrasse 42, 91054 Erlangen (Germany)

[†] Deceased.

[**] Transition-Metal Complexes with Sulfur Ligands, Part 168. For Part 167, see: D. Sellmann, R. Prakash, F. W. Heinemann, *Eur. J. Inorg. Chem.* **2004**, in press. '$N_2Me_2S_2$' = 1,2-ethanediamine-*N*,*N*′-dimethyl-*N*,*N*′-bis(2-benzenethiolate)(2−).

Introduction

Nitrogenases differ from many other enzymes in their versatility in catalyzing the reduction of not only one but numerous substrates. These substrates range from molecular nitrogen to protons, acetylene, nitriles, isonitriles, and even HCN.[1] All these reductions probably take place in $2H^+/2e^-$ transfer steps at the metal sulfur cofactors of nitrogenases.[2,3] The detailed mechanisms of these reactions have remained largely unknown, and model compounds that enable the catalytic reduction of nitrogenase substrates under mild, nitrogenase-like conditions are the goal of continual efforts.[4–6]

Among the nitrogenase substrates, protons and molecular hydrogen play a special role. Protons are reduced to H_2, and in this regard, nitrogenases exhibit hydrogenase activity. Although molecular hydrogen is a competitive inhibitor of N_2 fixation, it is also a substrate.[7] This is demonstrated by one

  DOI: 10.1002/chem.200400120

of the most intriguing nitrogenase reactions, that is, "N_2-dependent HD formation". This reaction involves the reductive formation of HD from D_2 and protons of water, which takes place exclusively in the presence of N_2. This reaction indicates that D_2 is heterolytically cleaved at the metal sulfur sites of the nitrogenase cofactors.[8] Because the active sites of nitrogenases are basically transition metal complexes with sulfur ligands, which react with nitrogenase substrates, low molecular weight metal–sulfur complexes are particularly desirable model compounds. In the search for such models we recently found the [Ru(P*i*Pr$_3$)('$N_2Me_2S_2$')] complex fragment (Scheme 1).[9]

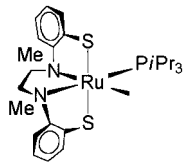

Scheme 1. The [Ru(P*i*Pr$_3$)('$N_2Me_2S_2$')] fragment.

The [Ru(P*i*Pr$_3$)('$N_2Me_2S_2$')] fragment can bind N_2 and other nitrogen ligands under ambient conditions, and it does not immediately block its vacant sites by formation of M-S-M bridges to give unreactive aggregates, which is a predominant feature of metal thiolates. On attempting to reduce the N_2 ligands in [Ru(N_2)(P*i*Pr$_3$)('$N_2Me_2S_2$')] (**1a**) and related complexes, we found that [Ru(PR$_3$)('$N_2Me_2S_2$')] fragments (R = *i*Pr, Cy) can also bind H_2, H^-, and BH_3. The resulting complexes are described here.

Results and Discussion

Synthesis of [Ru(L)(PR$_3$)('$N_2Me_2S_2$')] (L = η^2-H_2, BH_3, H^-; R = *i*Pr, Cy): Treatment of solutions of [Ru(N_2)(PR$_3$)('$N_2Me_2S_2$')] [**1a** (R = *i*Pr), **1b** (R = Cy)] in THF with molecular hydrogen led to a rapid color change from yellow-green to light red. Monitoring the reactions by IR spectroscopy showed that the ν(N≡N) bands of **1a** (2113 cm^{-1}) and **1b** (2115 cm^{-1}) decreased in intensity and had completely disappeared after 20 min. Concentration of the solutions and addition of MeOH or *n*-pentane precipitated yellow solids. They were completely characterized by elemental analysis, common spectroscopic methods, and X-ray crystal structure analysis as [Ru(H_2)(PR$_3$)('$N_2Me_2S_2$')] [**2a** (R = *i*Pr), **2b** (R = Cy)], which were formed according to Equation (1).

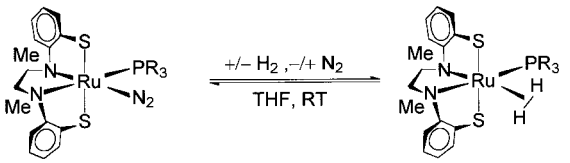

1a: R = *i* Pr
1b: R = Cy

2a: R = *i* Pr
2b: R = Cy

(1)

The ^{1}H NMR spectra of these η^2-H_2 complexes exhibit characteristic singlets at $\delta = -12.04$ (**2a**) and $\delta = -11.98$ ppm (**2b**), which are split by ^{31}P coupling into doublets [^2J(P,H) = 11.2 (**2a**), 9.2 Hz (**2b**)]. The stability of the η^2-H_2 complexes **2a** and **2b** is comparable to that of the corresponding N_2 complexes **1a** and **1b**. Since this was a quite unexpected result, DFT calculations were carried out. These calculations supported the experimental observations by showing that the bond enthalpy between [Ru(PR$_3$)('$N_2Me_2S_2$')] and H_2 and N_2 are almost identical (see Experimental Section). Both η^2-H_2 complexes **2a** and **2b** are stable in solution under an Ar/H_2 mixture for extended periods of time at room temperature, whereas solid, yellow **2a** and **2b** slowly turn green at room temperature due to loss of coordinated H_2. At −78 °C, however, they can be stored for months without decomposition. Replacing the gas phase of H_2 by N_2 led to regeneration of the N_2 complexes **2a** or **2b**, that is, the N_2/H_2 reaction of Equation (1) is reversible.

The dinuclear N_2 complex [μ-N_2{Ru(P*i*Pr$_3$)('$N_2Me_2S_2$')}$_2$] (**1c**) showed an analogous reaction towards H_2.[10] Treatment of **1c** with one equivalent of H_2 first resulted in the formation of the mononuclear N_2 complex [Ru(N_2)(P*i*Pr$_3$)('$N_2Me_2S_2$')] (**1a**) and **2a**. This result indicates that [μ-N_2{Ru(P*i*Pr$_3$)('$N_2Me_2S_2$')}$_2$] (**1c**) dissociated in solution to give mononuclear **1a** and the [Ru(P*i*Pr$_3$)('$N_2Me_2S_2$')] fragment, which instantaneously added H_2 [Eq. (2)].

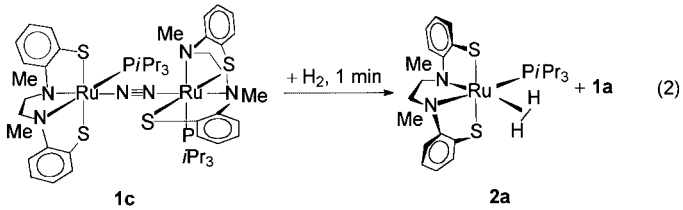

1c **2a** (2)

Further treatment of the solution with H_2 converted the initially formed [Ru(N_2)(P*i*Pr$_3$)('$N_2Me_2S_2$')] (**1a**) to the η^2-H_2 complex **2a**. η^2-H_2 complexes frequently exhibit strongly acidic H_2 ligands and are readily deprotonated to give hydride complexes.[11] However, all attempts to deprotonate **2a** or **2b** with bases such as LiOMe or LiN(SiMe$_3$)$_2$ were unsuccessful. For example, even when **2a** was treated with a 10- to 100-fold excess of LiN(SiMe$_3$)$_2$ in THF, no deprotonation of **2a** to give the corresponding hydride complex anion [Ru(H)(P*i*Pr$_3$)('$N_2Me_2S_2$')]$^-$ (**4a**) was observed, and **2a** could be recovered from the reaction solutions.

The ^{1}H and ^{31}P NMR spectra indicated the formation of additional decomposition products, which were not characterized. These findings indicated that the hydride complex anions [Ru(H)(PR$_3$)('$N_2Me_2S_2$')]$^-$ corresponding to **2a** or **2b** are extremely strong bases. The viability of such anions became evident when the reactions between **1a** or **1b** with borohydrides such as $NaBH_4$ and NBu_4BH_4 were investigated. Treatment of **1a** in THF with $NaBH_4$ did not lead to reduction of the N_2 ligand but to immediate evolution of gas and formation of orange solutions. Monitoring this reaction in [D_8]THF by ^{1}H, ^{11}B, and ^{31}P NMR spectroscopy showed that directly after combining **1a** and $NaBH_4$ one product was the η^2-H_2 complex **2a**, which was identified by its characteristic ^{1}H NMR signal at $\delta = -12.04$ ppm. Its formation

could be traced back to traces of moisture in the solvent (or on the glass walls) that reacted either with $NaBH_4$ or with a highly water sensitive species. The ^{31}P NMR spectrum showed that no N_2 complex **1a** remained, and that a second complex besides **2a** had formed, because a further ^{31}P NMR signal at $\delta = 55.55$ ppm was observed. However, the ^{11}B NMR spectrum showed a practically unchanged, but slightly broadened BH_4^- quintet, which suggested that BH_4^- ions were still present. These spectroscopic results are rationalized by the assumption that BH_4^- ions replaced the N_2 ligand of **1a** to give a very labile BH_4^- adduct $[Ru(BH_4)(PiPr_3)('N_2Me_2S_2')]^-$ showing a very weak interaction between the BH_4^- ion and the $[Ru(BH_4)(PiPr_3)('N_2Me_2S_2')]$ fragment [Eq. (3)].

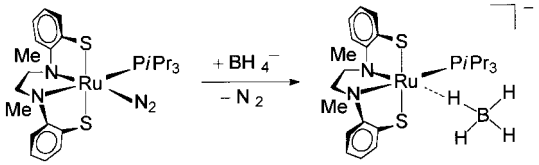

1a (3)

After several hours, an additional high-field ^1H NMR signal at $\delta = -18.13$ ppm indicated the presence of a third product with a hydride signal, tentatively assigned to a hydride complex or a derivative of the BH_4^- adduct. The ^{11}B NMR and mass spectra suggested the coordination not of BH_4^- but of BH_3 to the $[Ru(PiPr_3)('N_2Me_2S_2')]$ fragment. Slow diffusion of Et_2O into the filtered reaction solutions finally yielded a solid product in the form of single crystals whose X-ray crystal structure analysis substantiated the formation of $[Ru(BH_3)(PiPr_3)('N_2Me_2S_2')]$ (**3a**).

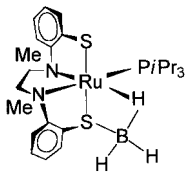

3a

When the mixture of **1a** and $NaBH_4$ in THF was kept for several days at room temperature, the ^1H NMR spectrum showed that the initially observed signal of the η^2-H_2 complex **2a** at $\delta = -12.04$ ppm had disappeared. The signal of **3a** at $\delta = -18.13$ ppm was still present, and, in addition to this signal, a new signal at even higher field ($\delta = -21.47$ ppm) had emerged (Figure 1).

The intensity of the signal at $\delta = -21.47$ ppm and its coupling constant of $^2J(P,H) = 38.4$ Hz were compatible with the formation of the monohydride complex anion $[Ru(H)(PiPr_3)('N_2Me_2S_2')]^-$. However, all attempts to isolate salts of this anion from the reaction solution were unsuccessful. The unambiguous identification of $[Ru(H)(PiPr_3)('N_2Me_2S_2')]^-$ (**4a**) was finally achieved by the complete characterization of $[Li(thf)_2][Ru(H)(PiPr_3)('N_2Me_2S_2')]$ ($[Li(thf)_2]$-**4a**), which was synthesized by a different route (see below).

Analogous results were obtained when the PCy_3 complex $[Ru(N_2)(PCy_3)('N_2Me_2S_2')]$ (**1b**) was treated with NBu_4BH_4 in THF. This experiment was done not only to probe the influence of the PCy_3 ligand versus that of $PiPr_3$, but also because it could be carried out in strictly homogenous phase, since NBu_4BH_4 is soluble in THF. The reaction between **1b** and NBu_4BH_4 also yielded the first single-crystalline example of the $[Ru(H)(PR_3)('N_2Me_2S_2')]^-$ complex type, in the form of $NBu_4[Ru(H)(PCy_3)('N_2Me_2S_2')]$ (NBu_4-**4b**). Complex NBu_4-**4b** could only be isolated in pure form when traces of water were strictly excluded. Otherwise, a second species, which was characterized as the BH_3 complex $[Ru(BH_3)(PCy_3)('N_2Me_2S_2')]$ (**3b**), is also formed.

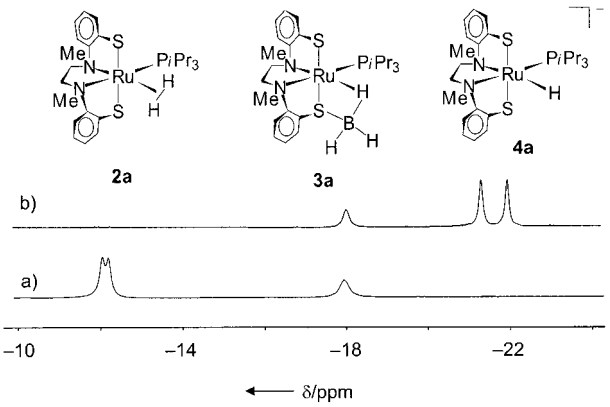

Figure 1. Monitoring the reaction between $[Ru(N_2)(PiPr_3)('N_2Me_2S_2')]$ (**1a**) and $NaBH_4$ in $[D_8]$THF by ^1H NMR spectroscopy. a) ^1H NMR spectrum indicating the formation of $[Ru(H_2)(PiPr_3)('N_2Me_2S_2')]$ (**2a**) and $[Ru(BH_3)(PiPr_3)('N_2Me_2S_2')]$ (**3a**); b) ^1H NMR spectrum after three days showing the additional formation of the $[Ru(H)(PiPr_3)('N_2Me_2S_2')]^-$ ion.

The unambiguous identification of the BH_3 complex $[Ru(BH_3)(PiPr_3)('N_2Me_2S_2')]$ [**3a** (R = *i*Pr), **3b** (R = Cy)] and the hydride complexes $[Li(thf)_2][Ru(H)(PiPr_3)('N_2Me_2S_2')]$ ($[Li(thf)_2]$-**4a**) and $NBu_4[Ru(H)(PCy_3)('N_2Me_2S_2')]$ (NBu_4-**4b**) prompted us to search for more rational and direct syntheses of these species by employing BH_3·THF and $LiBEt_3H$ as reagents. $LiBEt_3H$ was used instead of $NaBH_4$ or NBu_4BH_4 to avoid formation of BH_3 complexes **3a** and **3b**. These were formed as side products when $NaBH_4$ or NBu_4BH_4 was used as hydride source in the presence of residual traces of moisture (see above). As expected, treatment of the N_2 complexes **1a** or **1b** with BH_3·THF according to Equation (4) yielded the corresponding BH_3 complexes **3a** and **3b**, which were obtained in solid form and characterized by common spectroscopic methods.

$$\mathbf{1a},\mathbf{1b} + BH_3 \cdot THF \xrightarrow[-N_2]{} [Ru(BH_3)PR_3)(N_2Me_2S_2)] \quad \mathbf{3a}\ (R = iPr),\ \mathbf{3b}\ (R = Cy) \tag{4}$$

Treatment of the N_2 complexes **1a** or **1b** with $LiBEt_3H$ according to Equation (5) afforded the corresponding hydride complex anions **4a** and **4b**. However, this reaction pathway only yielded the $PiPr_3$ complex $[Li(thf)_2]$-**4a** in solid form. All attempts to isolate the PCy_3 analogue $[Li(thf)_2][Ru(H)(PCy_3)('N_2Me_2S_2')]$ ($[Li(thf)_2]$-**4b**) in crystalline form remained unsuccessful and always resulted in oily products that contained traces of unconverted $LiBEt_3H$.

$$\mathbf{1a},\mathbf{1b} + \mathrm{LiBEt_3H \cdot THF} \xrightarrow[-N_2]{} [\mathrm{Li(thf)_2}][\mathrm{Ru(H)(PR_3)(N_2Me_2S_2)}]$$
$$[\mathrm{Li(thf)_2}]\text{-}\mathbf{4a}\ (\mathrm{R} = i\mathrm{Pr})$$
$$[\mathrm{Li(thf)_2}]\text{-}\mathbf{4b}\ (\mathrm{R} = \mathrm{Cy}) \quad (5)$$

X-ray crystal structure analyses: Examples of the three types of complexes described in this paper could be characterized by X-ray crystal structure analysis. Figure 2 depicts

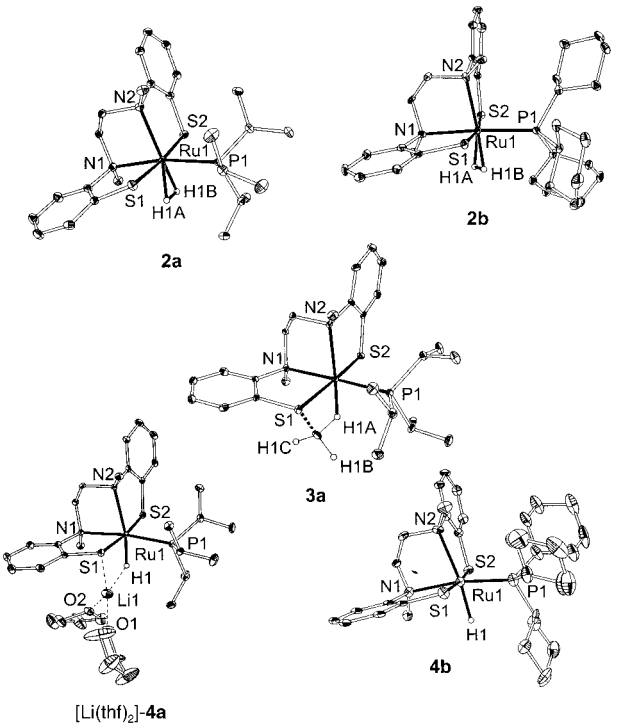

Figure 2. Molecular structures of $[Ru(H_2)(P\mathit{i}Pr_3)(\text{'}N_2Me_2S_2\text{'})]$ (**2a**), $[Ru(H_2)(PCy_3)(\text{'}N_2Me_2S_2\text{'})]\cdot 0.5$ pentane (**2b**·0.5 pentane), $[Ru(BH_3)(P\mathit{i}Pr_3)(\text{'}N_2Me_2S_2\text{'})]$ (**3a**), $[Li(THF)_2][Ru(H)(P\mathit{i}Pr_3)(\text{'}N_2Me_2S_2\text{'})]$ ($[Li(THF)_2]$**4a**), and $NBu_4[Ru(H)(PCy_3)(\text{'}N_2Me_2S_2\text{'})]\cdot 0.83\,Et_2O\cdot 0.17$ THF (NBu_4)**4b**·0.83 Et_2O·0.17 THF); (50% probability ellipsoids; solvent molecules, C-bonded H atoms, and NBu_4 cations omitted for clarity).

the molecular structures of **2a**, **2b**, **3a**, **4a**, and **4b**. Table 1 lists selected bond lengths and angles.

All complexes exhibit six-coordinate ruthenium centers in pseudo-octahedral coordination spheres and are C_1-symmetric. The '$N_2Me_2S_2$' ligand is coordinated to the metal centers in a helical mode that causes the thiolate donors to adopt *trans* positions. The crystal lattices of **2a**, **2b**, **3a**, and NBu_4-**4b** contain discrete molecules or cations and anions, and the crystal lattice of $[Li(thf)_2]$-**4a** contains ion pairs in which the $[Li(thf)_2]$ ions are bound to the $[Ru(H)(P\mathit{i}Pr_3)(\text{'}N_2Me_2S_2\text{'})]^-$ ions through Li···S–Ru and Li···H–Ru bridges.

The H^- ligands in the complex anions **4a** and **4b** result in particularly long Ru1–N2 distances, and **4b** (240.3(5) ppm) has a longer Ru1–N2 bond than **4a** (233.9(2) ppm). This may be traced back to the fact that **4b** has a terminal hydride ligand, while **4a** exhibits a hydride ligand bridging to the $[Li(thf)_2]$ entity. The Ru1–N2 distances in the η^2-H_2 complexes **2a** (227.7(2) ppm) and **2b** (222.1(4) ppm) are shorter than those in the hydride complex anions **4a** and **4b** and lie in the usual range of $[Ru(L)(PR_3)(\text{'}N_2Me_2S_2\text{'})]$ complexes. However, it is difficult to rationalize why the Ru1–N2 distance in **2b** is shorter than that in **2a**. Futhermore, the shorter the Ru1–P1 distances, the longer the Ru1–N2 distances. This possibly indicates that differences at the Ru centers caused by elongation of the Ru1–N2 bonds are counterbalanced by shortening of the Ru1–P1 bonds. This is most visible in the hydride complex anion **4b**, which has a very long Ru1–N2 distance (240.3(5) pm) and a very short Ru1–P1 distance (224.8(2) pm). The distances in the BH_3 complex **3a** lie in the usual range for $[Ru(L)(PR_3)(\text{'}N_2Me_2S_2\text{'})]$ complexes. The relatively short Ru1–N2 distance of **3a** (223.6(3) ppm) indicates the absence of a strong *trans* influence of the H1A atom of the BH_3 entity on the Ru1–N2 bond. The BH_3 entity apparently acts as a weak ligand, comparable to the weak η^2-H_2 ligands in **2a** and **2b**. The positions of the η^2-H_2, the hydrogen atoms of the BH_3 entity, and the hydride ligands in **2a**, **3a**, and **4a** could be determined from difference Fourier maps. The Ru–H distances lie in the usual range of 160–170 pm. Such distances are also found for related complexes, for example, $[Li(thf)(Et_2O)][Ru(H)(PCy_3)(\text{'}S_4\text{'})]$ ('S_4' = dianion of 1,2-bis(2-mercaptophenylthio)ethane; 161(5) pm) and $[Na(THF)][Ru(H)(\text{'}^{t\mathrm{bu}}pyS_4\text{'})]_2$ ('$^{t\mathrm{bu}}pyS_4$' = dianion of 2,6-bis[(2-mercapto-3,5-di-*tert*-butylphenylthio)dimethylpyridine]; 161(5) pm).[12,13] Relatively large standard deviations do not enable a detailed discussion of either Ru–H or H–H distances, but the quality of the single crystals of **2a** enabled localization of the η^2-H_2 ligand. The H–H distance was determined to be 92 pm, which is 18 pm longer than in the free H_2 molecule. This is in agreement with the value of 99 pm for **2a**, as calculated on the basis of the H,D coupling constant ($^1J(\mathrm{H,D}) = 26.0$ Hz, see also below) according to Equation (6).[11]

$$d_{\mathrm{H-H}}/\text{Å} = 1.42 - 0.0167\,\mathrm{J(H,D)} \quad (6)$$

The H–H distance in the related η^2-H_2 PCy_3 complex **2b** was determined to be 99 pm by X-ray crystal structure determination, which agreed with the value calculated from the H,D coupling constant (98 pm). The short elongation of the H–H bond in the η^2-H_2 ligands of **2a** and **2b** compared to the free H_2 molecule indicates only minor activation of these ligands. The B1–H1A distance (128(4) pm) of the H atom bound to the Ru center is significantly elongated in comparison to the terminal B–H bonds (B1–H1B 113(4) pm, B1–H1C 111(5) pm). The Ru–H1A distance is similar to those of classical hydride complexes. The terminal B–H bonds are similar to those of related systems.[14]

General properties and spectroscopic characterization of complexes 2–4: All complexes described here are yellow to orange and diamagnetic. They are soluble in THF, but only sparingly soluble in *n*-pentane or methanol. The H_2 ligands in the η^2-H_2 complexes **2a** and **2b** (as well as the N_2 ligands in the N_2 complexes **1a** and **1b**) are very labile. The dissociation of the H_2 (or N_2) ligands yields 16-valence-electron

Table 1. Selected bond lengths [pm] and angles [°] in **2a**, **2b**·0.5 pentane, **3a**, [Li(thf)$_2$]-**4a**, and NBu$_4$-**4b**·0.83 Et$_2$O·0.17 THF.

Complex	**2a**	**2b**	**3a**	**4a**	**4b**
Ru1–N1	224.0(2)	225.5(4)	227.8(3)	226.8(2)	226.9(5)
Ru1–N2	227.7(2)	222.1(4)	223.6(3)	233.9(2)	240.3(5)
Ru1–S1	238.2(1)	239.5(1)	236.4(1)	237.4(1)	236.0(2)
Ru1–S2	238.0(1)	238.6(1)	235.9(1)	237.1(1)	236.7(2)
Ru1–P1	232.1(1)	233.5(1)	233.3(1)	226.5(1)	224.8(2)
Ru1–H1(A)	164(3)	159.81	168(5)	161(4)	174(8)
Ru1–H1B	160(3)	168.99	–	–	–
S1–B1	–	–	193.2(4)	–	–
H1A–H1B	92	99	–	–	–
B1–H1A	–	–	128(4)	–	–
B1–H1B	–	–	113(4)	–	–
B1–H1C	–	–	111(5)	–	–
N1-Ru1-N2	81.2(1)	82.6(1)	81.3(1)	79.8(1)	79.0(2)
S1-Ru1-S2	174.5(1)	171.0(1)	168.3(1)	173.0(1)	173.0(1)
S1-Ru1-P1	93.5(1)	99.9(1)	96.1(1)	96.3(1)	94.0(1)
N1-Ru1-P1	170.2(1)	174.8(1)	178.1(1)	171.5(1)	170.0(1)
H1(A)-Ru1-N2	158.8(1)	165.1	171.9(15)	165.2(16)	170(3)
H1(A)-Ru1-S2	78.6(1)	111.0	92.0(15)	92.8(15)	95(2)
Li1–S1	–	–	–	239.7(6)	–
Li1–H1	–	–	–	193(4)	–
Li1–O1	–	–	–	197.7(6)	–
Li1–O2	–	–	–	195.4(6)	–

[Ru(PR$_3$)('N$_2$Me$_2$S$_2$')] (R = *i*Pr, Cy) fragments, which are most probably the reactive species in all reactions reported.

As was found for other complexes with H$^-$ ligands, the hydride complex anions [Ru(H)(PR$_3$)('N$_2$Me$_2$S$_2$')]$^-$ [**4a** (R = *i*Pr), **4b** (R = Cy)] are so strongly Brønsted basic that they instantaneously produce the corresponding η^2-H$_2$ complexes **2a** and **2b** if traces of moisture or other protic solvents, for example, MeOH, are present.[15]

The complexes are stable in solution for longer periods of time, and in the solid state the BH$_3$ complexes can be kept at room temperature without decomposition, whereas the η^2-H$_2$ complexes **2a** and **2b** and the hydride complexes [Li(thf)$_2$]-**4a** and NBu$_4$**4b** must be stored at −78 °C to prevent decomposition. The hydride complex anions **4a** and **4b** are extremely sensitive to moisture, both in the solid state and in solution.

The complexes were characterized by ^{1}H, ^{13}C, ^{31}P, and, in the case of **3a** and **3b**, also by ^{11}B NMR spectroscopy. All NMR spectra were in agreement with the structures determined by X-ray crystal structure analysis. The ^{1}H NMR spectra exhibit the typical pattern of complexes having the [Ru('N$_2$Me$_2$S$_2$')] core and phosphane co-ligands (Figure 3).

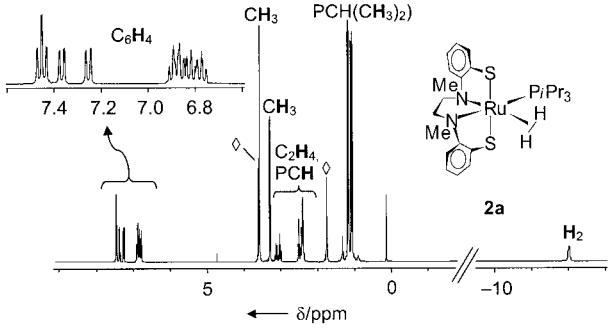

Figure 3. ^{1}H NMR spectrum of [Ru(H$_2$)(P*i*Pr$_3$)('N$_2$Me$_2$S$_2$')] (**2a**) in [D$_8$]THF; ◊ = [D$_8$]THF.

Two methyl signals of the *N*-methyl groups are particularly characteristic for the '$N_2Me_2S_2^{2-}$' ligand in C_1-symmetric [Ru(L)(PR$_3$)('N$_2$Me$_2$S$_2$')] complexes and complex anions. The η^2-H$_2$ and hydride ligands give rise to signals in the region of $\delta = -12.02$ (**2a**) and −11.98 ppm (**2b**), respectively, and at $\delta = -21.47$ (**4a**) and −21.83 ppm (**4b**). These signals are split into doublets with ^2J(P,H) = 11.2 (**2a**), 9.8 (**2b**), 38.4 (**4a**), and 32.8 Hz (**4b**). The large coupling constants of more than 30 Hz agree with the *cis* coordination of the hydride and phosphane co-ligands in **4a** and **4b**.[16] The BH$_3$ entities of the BH$_3$ complexes **3a** and **3b** give rise to two multiplets (due to ^{1}H,^{1}H, ^{31}P,^{1}H, and ^{11}B,^{1}H coupling) in the region of $\delta = -18.13$ (**3a**) and −18.14 ppm (**3b**), indicative of two types of B–H bonds. The high-field signals are assigned to B–H groups interacting with the Ru centers, and their shifts indicate B-H-Ru interactions that may be described as agostic or three-center, two-electron bonds. Particular emphasis was paid to corroborating the η^2-H$_2$ bonding mode of the H$_2$ ligands in **2a** and **2b** by NMR spectroscopy. Measurement of T_1 relaxation times afforded values of $T_1 = 35$ ms for **2a** and $T_1 = 21$ ms for **2b** (500 MHz spectrometer, 293 K) that are compatible with η^2-H$_2$ ligands.[17] Further proof for the η^2-H$_2$ bonding mode was obtained from the HD coupling constants in the analogous complexes [Ru(HD)(P*i*Pr$_3$)('N$_2$Me$_2$S$_2$')] (HD-**2a**) and [Ru(HD)(PCy$_3$)('N$_2$Me$_2$S$_2$')] (HD-**2b**). Complexes HD-**2a** and HD-**2b** were easily synthesized by reaction of N$_2$ complexes **1a** and **1b** with NaBD$_4$ in THF which contained stoichiometric quantities of H$_2$O as a source of H$^+$.

The complexes HD-**2a** and HD-**2b** show large coupling constants [^1J(H,D) = 26.0 (HD-**2a**) and 25.9 Hz (HD-**2b**)], which are unambiguous proof of activated, but still intact, H–D bonds.[18] Gaseous HD has ^1J(H,D) = 43.2 Hz, while *cis*-[M(H)(D)] complexes with hydride and deuteride ligands usually exhibit ^2J(H,D) < 2 Hz.[19]

The J(H,D) values found for HD-**2a** and HD-**2b** are also comparable with those of, for example, [W(HD)(CO)$_3$-(PCy$_3$)] (^1J(H,D) = 33.5 Hz).[20] Due to H,D and H,P coupling, the HD ligands of HD-**2a** and HD-**2b** give rise to a doublet of triplets in the ^{1}H NMR spectrum, which is shown for HD-**2a** in Figure 4.

The H,D coupling constants of 26.0 and 25.9 found for HD-**2a** and HD-**2b** enabled estimates of the H–D distances. They were calculated to be 98 pm according to Equation (6).[11] These values agree well with those derived from the X-ray crystal structure analyses of **2a** (92 pm) and **2b** (99 pm). Comparison of these distances with the bond length in free H$_2$ (74 pm) illustrates again that H$_2$ is rather

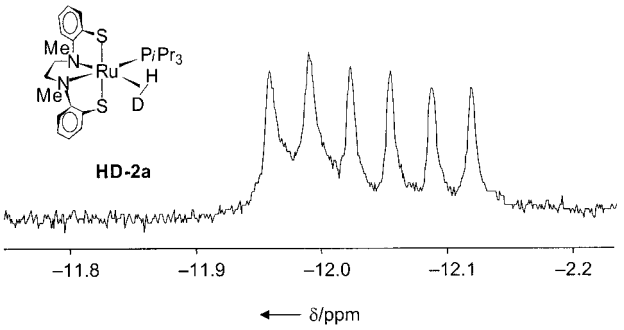

Figure 4. High-field region of the ^{1}H NMR spectrum of [Ru(HD)(P*i*Pr$_3$)('$N_2Me_2S_2$')] (HD-**2a**) in [D$_8$]THF.

weakly activated when bound to [Ru(PR$_3$)('$N_2Me_2S_2$')] fragments. In other nonclassical η^2-HD complexes, for example, [Cp*Ru(HD)(dppm)]BF$_4$ (Cp* = pentamethylcyclopentadienyl, dppm = bis(diphenylphosphanyl)methane) the activation of HD can be much stronger.[21]

Reactivity of η^2-H$_2$, BH$_3$, and H$^-$ complexes 2–4: The relatively weak activation of H$_2$ in **2a** and **2b** corresponds with the reactivity of these complexes towards deprotonation or substitution of the H$_2$ ligands. The related η^2-H$_2$ complex [Rh(H$_2$)(PCy$_3$)('^{bu}S$_4$')]$^+$ ('^{bu}S$_4$' = dianion of 1,2-bis(2-mercapto-3,5-di-*tert*-butylphenylthio)ethane) only exists as a transition state and immediately forms the thiol hydride complex [Rh(H)(PCy$_3$)('^{bu}S$_4$-H')]$^+$ (Scheme 2).[22]

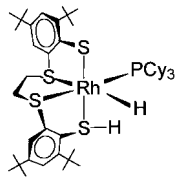

Scheme 2. [Rh(H)(PCy$_3$)('^{bu}S$_4$'-H)]

The η^2-H$_2$ complex [Ru(H$_2$)(PCy$_3$)('S$_4$')] ('S$_4$' = dianion of 1,2-bis[(2-mercaptophenylthio)ethane]), which is also related to **2a** and **2b**, is readily deprotonated by bases such as NaOMe to give [Ru(H)(PCy$_3$)('S$_4$')]$^-$.[12] In contrast, no such reaction could be observed for **2a** or **2b** (see above).

While H$_2$/N$_2$ exchange is reversible (see above), the H$_2$ ligands in **2a** or **2b** are instantaneously replaced by CO to give [Ru(CO)(PR$_3$)('$N_2Me_2S_2$')] [Equation (7)].

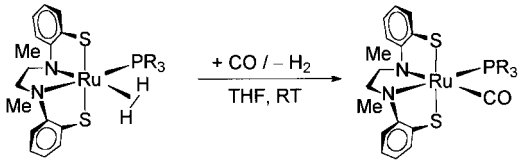

(7)

2a: R = *i*Pr
2b: R = Cy

The η^2-H$_2$ complexes **2a** and **2b** instantaneously react with BH$_3$·THF to give the borane complexes [Ru(BH$_3$)(PR$_3$)('$N_2Me_2S_2$')] [**3a** (R = *i*Pr), **3b** (R = Cy)]. Since substitution-inert [Ru(L)(PR$_3$)('$N_2Me_2S_2$')] complexes like [Ru(CO)(P*i*Pr$_3$)('$N_2Me_2S_2$')] or [Ru(PMe$_3$)$_2$('$N_2Me_2S_2$')] do not react with BH$_3$·THF, the formation of the borane complexes **3a** and **3b** is, similar to the reactions with BH$_4^-$ ions (see above), best rationalized by coordination of the BH$_3$ entity of the BH$_3$·THF adduct through one hydrogen atom to the [Ru(PR$_3$)('$N_2Me_2S_2$')] fragments as shown in Equation (8).[10,23]

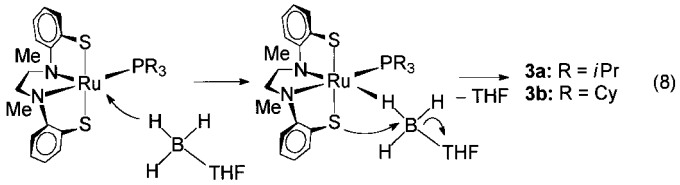

(8)

The formation of the BH$_3$ complexes probably involves a very labile [Ru(PR$_3$)('$N_2Me_2S_2$')][BH$_3$·THF] adduct (see above), which cannot be detected, since final formation of the BH$_3$ complexes **3** is facilitated by the Lewis-basic thiolate S donor in *cis* position.

In contrast to the H$_2$ (or N$_2$) complexes **2a**, **2b** (or **1a** and **1b**), which are labile with regard to the exchange of the H$_2$ (or N$_2$) ligands, the borane complexes [Ru(BH$_3$)(PR$_3$)('$N_2Me_2S_2$')] **3a** and **3b** are inert towards both H$_2$ and N$_2$. Even under an atmosphere of CO, the related CO complexes [Ru(CO)(PR$_3$)('$N_2Me_2S_2$')] (R = *i*Pr, Cy) were not formed.[10,23] These observations strongly suggest a stable three-center, two-electron bonding mode of the BH$_3$ entity to the Ru center, which blocks the sixth coordination site. However, the N$_2$ complexes **1a** and **1b** or the related CO complexes [Ru(CO)(PR$_3$)('$N_2Me_2S_2$')] (R = *i*Pr, Cy) are formed when **3a** or **3b** is treated with stoichometric quantities of HBF$_4$ under an atmosphere of N$_2$ or CO. Carrying out these reactions under an atmosphere of argon led to quantitative formation of the η^2-H$_2$ complexes **2a** and **2b**. These observations are rationalized best by a reaction of protons with the BH$_3$ entity to give H$_2$. Subsequent substitution of the resulting BH$_2$ entity (which probably finally forms insoluble boranes B$_x$H$_y$) by H$_2$ leads to formation of the H$_2$ complexes **2a** and **2b** (Scheme 3).

The high stability of the Ru-H-B bond also explains why no further reaction of the borane complexes **3a** and **3b** with excess BH$_3$·THF was observed. This is due to the lack of a free coordination site at the Ru center in the borane complexes.

Reaction pathways leading from the N$_2$ complexes 1a or 1b to the H$_2$, H$^-$, or BH$_3$ complexes 2–4: The lability of the N$_2$ ligands in [Ru(N$_2$)(PR$_3$)('$N_2Me_2S_2$')] [**1a** (R = *i*Pr), **1b** (R = Cy)], the comparably ready dissociation of the H$_2$ ligands in **2a** or **2b**, and the extreme basicity of the hydride ligands in **4a** or **4b** enable a plausible description for the reactions of **1a** or **1b**, with H$_2$, NaBH$_4$, NBu$_4$BH$_4$, LiBEt$_3$H, or BH$_3$·THF (Scheme 4).

The initial step of the reaction of **1** with H$_2$, BH$_3$, BH$_4^-$ (or BEt$_3$H$^-$) is the dissociation of the N$_2$ ligand to give coordinatively unsaturated [Ru(PR$_3$)('$N_2Me_2S_2$')] (R = *i*Pr, Cy) fragments. These fragments react with H$_2$ to directly give

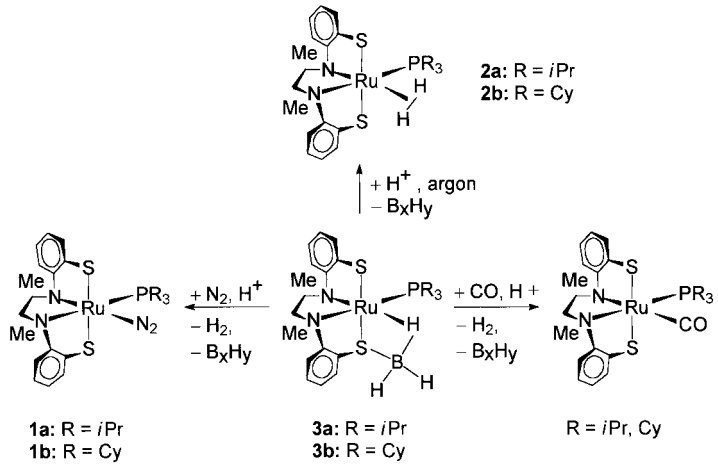

Scheme 3. Reactions of the borane complexes $[Ru(BH_3)(PR_3)('N_2Me_2S_2')]$ [**3a** (R = *i*Pr), **3b** (R = Cy)].

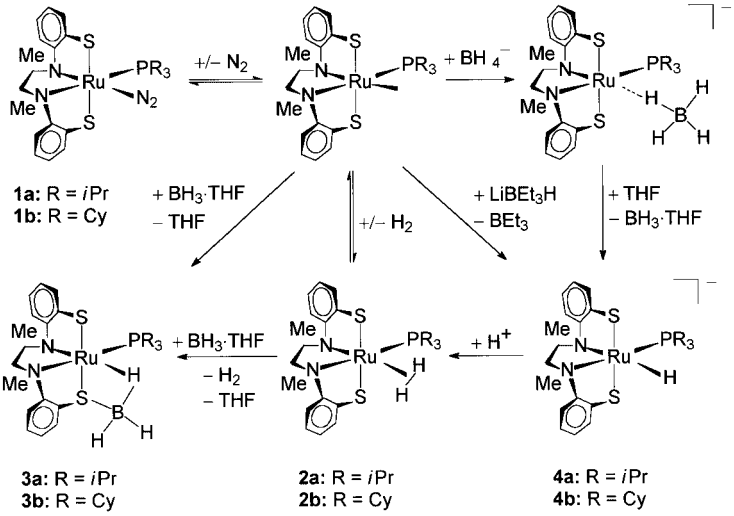

Scheme 4. Reaction pathways leading to the formation of $[Ru(H_2)(PR_3)('N_2Me_2S_2')]$ [**2a** (R = *i*Pr), **2b** (R = Cy)], $[Ru(BH_3)(PR_3)('N_2Me_2S_2')]$ [**3a** (R = *i*Pr), **3b** (R = Cy)], and $[Ru(H)(PR_3)('N_2Me_2S_2')]^-$ [**4a** (R = *i*Pr), **4b** (R = Cy)].

the η^2-H_2 complexes **2**, and with BH_3·THF to form the BH_3 complexes **3**.

With BH_4^-, either from $NaBH_4$ or NBu_4BH_4, the $[Ru(PR_3)('N_2Me_2S_2')]$ fragments most likely give BH_4^- adducts of the $[Ru(BH_4)(PR_3)('N_2Me_2S_2')]^-$ type. Rapid decomposition of the BH_4^- adducts affords the hydride complexes **4a** and **4b**. If moisture is not strictly excluded, the hydride complexes instantaneously react with protons to give the η^2-H_2 complexes **2a** and **2b**.

The direct reaction of the $[Ru(PR_3)('N_2Me_2S_2')]$ (R = *i*Pr, Cy) fragments with the hydride source $LiBEt_3H$ in rigorously dried solvents and glassware explains the rational synthesis of the hydride complex anions **4**. Even in the presence of traces of water, no borane complexes of the general formula $[Ru(BEt_3)(PR_3)('N_2Me_2S_2')]$ are formed, since BEt_3 is probably not prone to form stable three-center two-electron C–H–Ru bonds.

Conclusion

We have described the synthesis and characterization of complexes in which η^2-H_2, H^-, and BH_3 ligands bind to $[Ru(PR_3)('N_2Me_2S_2')]$ complex fragments. The resultant complexes demonstrate the unique capability of $[Ru(PR_3)('N_2Me_2S_2')]$ fragments to bind nitrogenase-relevant species to identical transition metal–sulfur sites, and these species now range from CO, N_2, N_2H_2, N_2H_4, NH_3, to hydride and H_2.[9,10,23,24] All these species interact with the metal–sulfur cofactors of nitrogenases or are assumed to be essential intermediates in the reduction of N_2 to NH_3. The coordination of η^2-H_2 and N_2 ligands to the $[Ru(PR_3)('N_2Me_2S_2')]$ fragments corresponds with previous findings showing that metal complex fragments can bind H_2 if the corresponding N_2 complexes exhibit $\nu(N{\equiv}N)$ bands in the region between 2160 and 2060 cm^{-1}, as do $[Ru(N_2)(P\mathit{i}Pr_3)('N_2Me_2S_2')]$ (**1a**) (2111 cm^{-1}) and $[Ru(N_2)(PCy_3)('N_2Me_2S_2')]$ (**1b**) (2113 cm^{-1}).[25] However, the $[Ru(L)(PR_3)('N_2Me_2S_2')]$ complexes **1a**/**1b** and **2a**/**2b** are the first examples proving that this relationship also holds for transition-metal thiolate complexes that can bind and activate H_2.[12,22] In the few known cases, the interaction between H_2 and the transition metal thiolate site favors the heterolysis of H_2 through the concerted attack of the Lewis-acidic metal centers and Brønsted-basic thiolate donors on the H–H bond. No such reaction could be observed with the η^2-H_2 complexes **2a** and **2b**, which may be rationalized by the fact that the η^2-H_2 ligand is only weakly activated in **2a** and **2b** and by the extreme Brønsted basicity of the hydride anions $[Ru(H)(PR_3)('N_2Me_2S_2')]^-$ (**4a**, **4b**).

The BH_3 complexes $[Ru(BH_3)(PR_3)('N_2Me_2S_2')]$ (**3a**, **3b**) are rare examples of transition metal BH_3 complexes, and, to the best of our knowledge, the first examples of BH_3 complexes of metal–sulfur complex fragments. The BH_3 ligands in these complexes bind to the $[Ru(PR_3)('N_2Me_2S_2')]$ fragments through two types of Lewis acid–base interactions yielding S–B and H–Ru bonds. This type of bonding contrasts with the bonds found in transition metal complexes of BH_4^-, such as $[Cu(PPh_3)_2(BH_4)]$, $[Cp_2Ti(BH_4)]$, and $[Zr(BH_4)_3]$, in which the BH_4^- ion binds to the metal centers through one or two B–H···M hydrogen bonds.[26,27,28]

Experimental Section

General: Unless noted otherwise, all reactions and spectroscopic measurements were carried out at room temperature under argon or nitrogen using standard Schlenk techniques in absolute solvents purchased from Fluka or Acros Chemicals. As far as possible, all reactions were monitored by IR and NMR spectroscopy. IR spectra in solution were recorded in CaF_2 cuvettes with compensation of the solvent bands; solids were measured as KBr pellets. NMR spectra were recorded, unless otherwise specified, at room temperature (20 °C) in the solvents indicated. Chemical shifts are given in ppm and reported relative to residual protonated solvent resonances (^1H, ^{13}C) or external standards: BF_3·Et_2O (^{11}B), H_3PO_4 (^{31}P). Relaxation times T_1 were measured on a JEOL Alpha 500 instrument at 500 MHz by the inversion recovery method with a standard pulse frequency (180°–τ–90°–FID). Mass spectra were measured in the field-desorption (FD) mode. The physical measurements were carried out with the following instruments: IR spectroscopy: Perkin-Elmer 983,

Perkin-Elmer 1600 FTIR, and Perkin-Elmer 16PC FTIR; NMR spectroscopy: JEOL FT-JNM-GX 270, Lambda LA 400, JEOL Alpha 500; mass spectrometry: Jeol MSTATION 700; Raman spectroscopy: Bruker FT-Raman RFS100/S.

The synthesis of $[Ru(N_2)(PR_3)('N_2Me_2S_2')]$ [R = *i*Pr (**1b**), Cy (**2b**)][9,23] was performed as described in the literature; NBu_4BH_4, $NaBH_4$, $NaBD_4$ were obtained from Aldrich, and $LiBEt_3H$ (1 M in THF) and BH_3·THF (1 M in THF) from Acros Chemicals.

[Ru(H$_2$)(PR$_3$)('N$_2$Me$_2$S$_2$')], general method: An intense stream of H_2 gas was passed through yellow solutions of $[Ru(N_2)(PR_3)('N_2Me_2S_2')]$ [**1a** (R = *i*Pr), **1b** (R = Cy)] in THF (30 mL) for 30 min. The reactions were monitored by IR spectroscopy and terminated when the ν(N≡N) band of **1a** (2113 cm^{-1}) or **1b** (2115 cm^{-1}) had disappeared. The red-green solutions were filtered and reduced in volume to 2 mL by a stream of hydrogen gas. Addition of hydrogen-saturated *n*-pentane (30 mL) yielded pale yellow solids, which were separated after 30 min, washed with hydrogen-saturated *n*-pentane (10 mL), and dried in vacuo for 1 h.

[Ru(H$_2$)(P*i*Pr$_3$)('N$_2$Me$_2$S$_2$')] (2a): $[Ru(N_2)(PiPr_3)('N_2Me_2S_2')]$ (**1a**) (300 mg, 0.51 mmol). Yield: 250 mg (87%) of $[Ru(H_2)(PiPr_3)('N_2Me_2S_2')]$ (**2a**); ^{1}H NMR (399.65 MHz, [D$_8$]THF): $\delta = 7.44$ (d, $^3J(H,H) = 7.0$ Hz, 1H, C_6H_4), 7.42 (d, $^3J(H,H) = 7.0$ Hz, 1H, C_6H_4), 7.34 (d, $^3J(H,H) = 8.0$ Hz, 1H, C_6H_4), 7.23 (d, $^3J(H,H) = 8.4$ Hz, 1H, C_6H_4), 6.89–6.69 (m, 4H, C_6H_4), 3.56 (s, 3H, CH_3), 3.28 (s, 3H, CH_3), 3.27–2.48 (m, 4H, C_2H_4), 2.45–2.33 (m, 3H, P[C*H*$(CH_3)_2]_3$), 1.17–1.21 (m, 9H, P[CH($CH_3)_2]_3$), −12.04 ppm (d, $^2J(P,H) = 11.2$ Hz, 2H, H_2); ^{13}C{^{1}H} NMR (100.40 MHz, [D$_8$]THF): $\delta = 153.6$, 153.4, 153.2, 152.8, 132.0, 131.7, 126.8, 126.7, 122.2, 121.7, 121.6, 121.5 (C_6H_4), 68.6, 62.7 (CH_3), 52.4, 50.9 (C_2H_4), 26.9 (d, $^1J(P,C) = 20.7$ Hz, P[*C*H$(CH_3)_2]_3$), 20.5, 20.1 ppm (P[CH($CH_3)_2]_3$); ^{31}P{^{1}H} NMR (161.70 MHz, [D$_8$]THF): $\delta = 59.11$ ppm ($P[C_3H_7]_3$); MS (^{102}Ru, THF): *m*/*z*: 564 [$M^+ - H_2$]; elemental analysis calcd (%) for $C_{25}H_{41}N_2RuPS_2$ (565.76): C 53.07, H 7.30, N 4.95, S 11.34; found: C 53.42, H 7.66, N 5.09, S 11.24.

[Ru(H$_2$)(PCy$_3$)('N$_2$Me$_2$S$_2$')] (2b): $[Ru(N_2)(PCy_3)('N_2Me_2S_2')]$ (**1b**) (440 mg, 0.62 mmol). Yield: 380 mg (90%) of $[Ru(H_2)(PCy_3)('N_2Me_2S_2')]$ (**2b**); ^{1}H NMR (399.65 MHz, [D$_8$]THF): $\delta = 7.47$–7.43 (m, 2H, C_6H_4), 7.33 (d, $^3J(H,H) = 8.4$ Hz, 1H, C_6H_4), 7.22 (d, $^3J(H,H) = 7.2$ Hz, 1H, C_6H_4), 6.88–6.73 (m, 4H, C_6H_4), 3.54 (s, 3H, CH_3), 3.28 (s, 3H, CH_3), 3.16–2.36 (m, 4H, C_2H_4), 2.20–2.12 (m, 3H, P[C*H*$(C_5H_{10})]_3$), 1.98–1.06 (m, 30H, P[CH($C_5H_{10})]_3$), −11.98 ppm (d, $^2J(P,H) = 9.2$ Hz, 2H, H_2); ^{13}C{^{1}H} NMR (100.40 MHz, [D$_8$]THF): $\delta = 153.1$, 152.7, 152.3, 131.6, 131.2, 126.3, 126.2, 121.6, 121.0 (3 signals, C_6H_4), 68.3, 62.1 (CH_3), 52.3, 50.5 (C_2H_4), 36.9 (d, $^1J(P,C) = 20.2$ Hz, P[*C*H$(C_5H_{10})]_3$), 30.3, 30.1, 28.2, 28.1, 27.1 ppm (P[CH($C_5H_{10})]_3$); ^{31}P{^{1}H} NMR (161.70 MHz, [D$_8$]THF): $\delta = 50.35$ ppm ($P[C_6H_{11}]_3$); MS (^{102}Ru, THF): *m*/*z*: 684 [$M^+ - H_2$]; elemental analysis calcd (%) for $C_{34}H_{53}N_2RuPS_2$ (685.98): C 59.53, H 7.79, N 4.08, S 9.35; found: C 59.47, H 7.61, N 4.19, S 9.19.

[Ru(HD)(PR$_3$)('N$_2$Me$_2$S$_2$')] (NMR experiments), general method: Two equivalents of $NaBD_4$ were added to yellow solutions of $[Ru(N_2)(PR_3)('N_2Me_2S_2')]$ [**1a** (R = *i*Pr), **1b** (R = Cy)] and one equivalent of H_2O in [D$_8$]THF and stirred for 1 h. The resulting orange solutions were directly investigated by ^{1}H NMR spectroscopy, and HD coupling constants of HD-**2a** and HD-**2b** were determined.

[Ru(HD)(P*i*Pr$_3$)('N$_2$Me$_2$S$_2$')] (HD-2a): $[Ru(N_2)(PiPr_3)('N_2Me_2S_2')]$ (**1a**) (40 mg, 0.068 mmol), $NaBD_4$ (5.7 mg, 0.136 mmol), H_2O (1.2 μL, 0.068 mmol), [D$_8$]THF (0.6 mL).^{1}H NMR (399.65 MHz, [D$_8$]THF): $\delta = -12.04$ ppm (dt, $^1J(H,D) = 26.0$ Hz, $^2J(P,H) = 12.03$ Hz, 1H, *H*D).

[Ru(HD)(PCy$_3$)('N$_2$Me$_2$S$_2$')] (HD-2b): $[Ru(N_2)(PCy_3)('N_2Me_2S_2')]$ (**1b**) (36 mg, 0.051 mmol), $NaBD_4$ (4.3 mg, 0.102 mmol), H_2O (0.9 μL, 0.051 mmol), [D$_8$]THF (0.6 mL). ^{1}H NMR (399.65 MHz, [D$_8$]THF): $\delta = -12.01$ ppm (dt, $^1J(H,D) = 25.9$ Hz, $^2J(P,H) = 12.03$ Hz ,1H, *H*D).

[Ru(BH$_3$)(PR$_3$)('N$_2$Me$_2$S$_2$')], general method: Addition of a slight excess (1.2 equiv) of BH_3·THF (1 M solution in THF) to yellow solutions of $[Ru(N_2)(PR_3)('N_2Me_2S_2')]$ [**1a** (R = *i*Pr), **1b** (R = Cy)] in THF (35 mL) resulted in gas evolution and formation of yellow solutions within 1 h. The reaction solutions were filtered after 24 h and reduced in volume to 2 mL. Addition of *n*-pentane (40 mL) yielded yellow solids, which were washed with *n*-pentane (20 mL) and dried in vacuo.

[Ru(BH$_3$)(P*i*Pr$_3$)('N$_2$Me$_2$S$_2$')] (3a): $[Ru(N_2)(PiPr_3)('N_2Me_2S_2')]$ (**1a**) (420 mg, 0.71 mmol), BH_3·THF (0.85 mL, 0.85 mmol). Yield: 350 mg (76%) of $[Ru(BH_3)(PiPr_3)('N_2Me_2S_2')]$·THF (**3a**·THF); ^{1}H NMR (399.65 MHz, [D$_8$]THF): $\delta = 7.74$ (d, $^3J(H,H) = 7.6$ Hz, 1H, C_6H_4), 7.50–7.45 (m, 2H, C_6H_4), 7.25–7.21 (m, 1H, C_6H_4), 7.14–7.10 (m, 1H, C_6H_4), 6.87–6.76 (m, 2H, C_6H_4), 3.60 (s, 3H, CH_3), 3.10 (s, 3H, CH_3), 3.37–2.51 (m, 4H, C_2H_4), 2.13–2.04 (m, 3H, P[C*H*$(CH_3)_2]_3$), 1.79–1.76 (m, 1H, BH_3), 1.34–1.31 (m, 1H, BH_3), 1.29 –1.24 (m, 9H, P[CH($CH_3)_2]_3$), −18.13 ppm (br, 1H, Ru*H*BH_2); ^{11}B{^{1}H} (128.15 MHz, [D$_8$]THF): $\delta = -7.56$ ppm (s, BH_3); ^{13}C{^{1}H} NMR (100.40 MHz, [D$_8$]THF): $\delta = 154.7$, 153.2, 152.0, 145.3, 132.1, 131.7, 128.0, 126.9, 126.0, 124.6, 121.0, 119.4 (C_6H_4), 70.0, 60.7 (CH_3), 57.5, 49.1 (C_2H_4), 28.7 (d, $^1J(P,C) = 19.1$ Hz, P[*C*H$(CH_3)_2]_3$), 21.4, 19.4 ppm (P[CH(*C*$H_3)_2]_3$); ^{31}P{^{1}H} NMR (161.70 MHz, [D$_8$]THF): $\delta = 49.81$ ppm ($P[C_3H_7]_3$); IR (KBr): $\tilde{\nu} = 2443$, 2411 (B–H), 1796 cm^{-1} (Ru–H); MS (^{102}Ru, THF): *m*/*z*: 578 [M^+]; elemental analysis calcd (%) for $BC_{29}H_{50}N_2OPRuS_2$ (649.71): C 53.61, H 7.76, N 4.31, S 9.87; found: C 53.99, H 7.90, N 4.53, S 10.10.

[Ru(BH$_3$)(PCy$_3$)('N$_2$Me$_2$S$_2$')] (3b): $[Ru(N_2)(PCy_3)('N_2Me_2S_2')]$ (**1b**) (420 mg, 0.59 mmol), BH_3·THF (0.71 mL, 0.71 mmol). Yield: 350 mg (88%) of $[Ru(BH_3)(PCy_3)('N_2Me_2S_2')]$ (**3b**); ^{1}H NMR (399.65 MHz, [D$_8$]THF): $\delta = 7.77$ (d, $^3J(H,H) = 7.6$ Hz, 1H, C_6H_4), 7.49–7.21 (m, 1H, C_6H_4), 7.12 (d, $^3J(H,H) = 8.4$ Hz, 1H, C_6H_4), 6.90–6.73 (m, 2H, C_6H_4), 6.87–6.76 (m, 2H, C_6H_4), 3.63 (s, 3H, CH_3), 3.07 (s, 3H, CH_3), 3.28–2.30 (m, 4H, C_2H_4), 2.60–2.45 (m, 3H, P[C*H*$(C_5H_{10})]_3$), 1.79–1.07 (m, 32H, P[CH($C_5H_{10})]_3$), BH_3), −18.14 ppm (b, 1H, Ru*H*BH_2); ^{11}B{^{1}H} (128.15 MHz, [D$_8$]THF): $\delta = 20.54$ ppm (s, BH_3); ^{13}C{^{1}H} NMR (100.40 MHz, [D$_8$]THF): $\delta = 155.1$, 153.7, 152.7, 145.7, 132.7, 132.3, 128.5, 127.3, 126.7, 125.1, 121.5, 119.8 (C_6H_4), 70.7, 61.0 (CH_3), 57.7, 49.6 (C_2H_4), 39.5 (br, P[*C*H$(C_5H_{10})]_3$), 31.83 (2 signals), 28.3, 28.2, 27.7 ppm (P[CH($C_5H_{10})]_3$); ^{31}P{^{1}H} NMR (161.70 MHz, [D$_8$]THF): $\delta = 42.44$ ppm ($P[C_6H_{11}]_3$); IR (KBr): $\tilde{\nu} = 2437$ (br, B–H), 1792 cm^{-1} (Ru–H); MS (^{102}Ru, THF): *m*/*z*: 699 [M^+]; elemental analysis calcd (%) for $BC_{34}H_{54}N_2PRuS_2$ (697.80): C 58.52, H 7.80, N 4.01, S 9.19; found: C 59.00, H 7.94, N 4.00, S 8.89.

[Li(thf)$_2$][Ru(H)(P*i*Pr$_3$)('N$_2$Me$_2$S$_2$')] ([Li(thf)$_2$]4a): Addition of 2 equiv of $LiBEt_3H$ (0.68 mL of a 1 M solution in THF, 0.68 mmol) to a yellow solution of $[Ru(N_2)(PiPr_3)('N_2Me_2S_2')]$ (**1a**; 200 mg, 0.34 mmol) in THF (15 mL) resulted in gas evolution and formation of a yellow solution, which was stirred for 24 h. The solution was reduced in volume to 1 mL and filtered. On layering with Et_2O (5 mL), orange crystals formed over four weeks at −34 °C. They were separated at −78 °C and dried without further washing at −78 °C. Yield: 100 mg (41%) of $[Li(thf)_2][Ru(H)(PiPr_3)('N_2Me_2S_2')]$ ([Li(thf)$_2$]-**4a**); ^{1}H NMR (399.65 MHz, [D$_8$]THF): $\delta = 7.35$ (d, $^3J(H,H) = 7.6$ Hz, 1H, C_6H_4), 7.28 (d, $^3J(H,H) = 7.2$ Hz, 1H, C_6H_4), 7.17 (d, $^3J(H,H) = 7.2$ Hz, 1H, C_6H_4), 7.05 (d, $^3J(H,H) = 7.6$ Hz, 1H, C_6H_4), 6.17–6.45 (m, 4H, C_6H_4), 3.39 (s, 3H, CH_3), 3.29 (s, 3H, CH_3), 3.23–2.20 (m, 4H, C_2H_4), 2.34–2.12 (m, 3H, P[C*H*$(CH_3)_2]_3$), 1.12–1.07 (m, 9H, P[CH($CH_3)_2]_3$), 0.99–0.95 (m, 9H, P[CH($CH_3)_2]_3$), −21.47 ppm (d, $^2J(P,H) = 38.4$ Hz, 1H, RuH); ^{13}C{^{1}H} NMR (100.40 MHz, [D$_8$]THF): $\delta = 163.4$, 160.2, 157.5, 155.6, 134.4, 134.3, 126.8, 126.2, 124.1, 122.7, 121.3, 120.5 (C_6H_4), 68.9, 64.8 (CH_3), 54.8, 52.5 (C_2H_4), 30.2 (d, $^1J(P,C) = 16.5$ Hz, P[*C*H$(CH_3)_2]_3$), 22.8, 22.7 ppm (P[CH(*C*$H_3)_2]_3$); ^{31}P{^{1}H} NMR (161.70 MHz, [D$_8$]THF): $\delta = 79.88$ ppm (*P*$[C_3H_7]_3$); elemental analysis calcd (%) for $C_{33}H_{56}LiN_2O_2PRuS_2$ (715.90): C 55.37, H 7.88, N 3.91, S 8.96; found: C 55.06, H 7.86, N 4.02, S 8.86.

NBu$_4$[Ru(H)(PCy$_3$)('N$_2$Me$_2$S$_2$')] (NBu$_4$-4b): NBu_4BH_4 (2 equiv; 108 mg, 0.42 mmol) were added to a yellow solution of $[Ru(N_2)(PCy_3)('N_2Me_2S_2')]$ (**1b**) (150 mg, 0.21 mmol) in THF (15 mL) and stirred for 1 h. An orange solution formed, which was stirred for 24 h, filtered, reduced in volume to 1 mL, and layered with Et_2O (4 mL). Over two weeks orange crystals precipitated, which were separated and dried in vacuo without any further washing. Yield: 150 mg (71%) of NBu_4-$[Ru(H)(PCy_3)('N_2Me_2S_2')]$·0.83 Et_2O·0.17 THF (NBu_4**4b**·0.83 Et_2O·0.17 THF); ^{1}H NMR (399.65 MHz, [D$_8$]THF): $\delta = 7.44$ (d, $^3J(H,H) = 6.4$ Hz, 1H, C_6H_4), 7.35 (d, $^3J(H,H) = 6.8$ Hz, 1H, C_6H_4), 7.25 (d, $^3J(H,H) = 7.6$ Hz, 1H, C_6H_4), 6.70–6.68 (m, 2H, C_6H_4), 6.55–6.68 (m, 2H, C_6H_4), 3.40 (s, 3H, CH_3), 3.38 (t, $^3J(H,H) = 8.4$ Hz, 8H, $N[CH_2CH_2CH_2CH_3]_4^+$), 3.30 (s, 3H, CH_3), 3.27–2.16 (m, 4H, C_2H_4), 2.10–2.00 (m, 3H, P[C*H*$(C_5H_{10})]_3$), 1.70 (m, 8H, $N[CH_2CH_2CH_2CH_3]_4^+$), 1.45 (m, 8H, $N[CH_2CH_2CH_2CH_3]_4^+$), 0.99 (t, $^3J(H,H) = 7.2$ Hz, 12H, $N[CH_2CH_2CH_2CH_3]_4^+$), 1.70–0.8 (m, 30H, P[CH($C_5H_{10})]_3$), −21.83 ppm (d, $^2J(P,H) = 32.8$ Hz, 1H, RuH); ^{13}C{^{1}H} NMR (100.40 MHz, [D$_8$]THF): $\delta = 161.1$, 156.3, 155.6, 153.8, 133.0, 132.8, 125.7, 124.8, 123.0, 121.1, 120.8,

119.3 (C_6H_4), 66.7, 62.4 (CH_3), 59.03 ($N[CH_2CH_2CH_2CH_3]_4^+$), 58.80 ($N[CH_2CH_2CH_2CH_3]_4^+$), 52.3, 50.0 (C_2H_4), 39.9 (d, $^1J(P,C) = 15.3$ Hz, $P[CH(C_5H_{10})]_3$), 30.7, 29.2, 28.9, 27.7 (2 signals, $P[CH(C_5H_{10})]_3$), 20.21 ($N[CH_2CH_2CH_2CH_3]_4^+$), 13.74 ppm ($N[CH_2CH_2CH_2CH_3]_4^+$); $^{31}P\{^1H\}$ NMR (161.70 MHz, [D$_8$]THF): $\delta = 68.48$ ppm ($P[C_6H_{11}]_3$); elemental analysis calcd (%) for $C_{54}H_{97.66}N_3PRuS_2$ (1001.17): C 64.78, H 9.82, N 4.20, S 6.41; found: C 64.87, H 10.00, N 4.07, S 6.11.

[Li(thf)$_2$][Ru(H)(PCy$_3$)('N$_2$Me$_2$S$_2$')] ([Li(thf)$_2$]-4b): Addition of 2 equiv of $LiBEt_3H$ (0.14 mL of a 1 M solution in THF, 0.14 mmol) to a yellow solution of [Ru(N$_2$)(PCy$_3$)('N$_2$Me$_2$S$_2$')] (**1b**; 50 mg, 0.07 mmol) in THF (5 mL) resulted in gas evolution and formation of a yellow solution, which was stirred for 24 h. The solution was filtered and all solvents were evaporated. The crude product, which still contained unconsumed $LiBEt_3H$, was dissolved in [D$_8$]THF (0.8 mL), and formation of the $[Ru(H)(PCy_3)('N_2Me_2S_2')]^-$ (**4b**) was corroborated by ^1H, ^{13}C, and ^{31}P NMR spectroscopy.

Reaction of [Ru(N$_2$)(P*i*Pr$_3$)('N$_2$Me$_2$S$_2$')] (1a) with NaBH$_4$ and H$_2$O: 2 equiv of $NaBH_4$ (13 mg, 0.34 mmol) were added to a yellow solution of [Ru(N$_2$)(P*i*Pr$_3$)('N$_2$Me$_2$S$_2$')] (**1a**) (100 mg, 0.17 mmol) and H_2O (3.6 μL, 0.17 mmol) in THF (20 mL) and stirred for 1 h. An orange solution formed, which was stirred for 24 h, filtered, reduced in volume to 1 mL, and layered with Et_2O (4 mL). Over three weeks, orange crystals of [Ru(BH$_3$)(P*i*Pr$_3$)('N$_2$Me$_2$S$_2$')] (**3a**) precipitated, which were collected and dried in vacuo without any further washing. Yield: 40 mg (41 %) of [Ru(BH$_3$)(P*i*Pr$_3$)('N$_2$Me$_2$S$_2$')] (**3a**).

X-ray crystal structure analysis of 2a, 2b, 3a, 4a, and 4b: Red prisms of [Ru(H$_2$)(P*i*Pr$_3$)('N$_2$Me$_2$S$_2$')] (**2a**) were obtained over two weeks at room temperature on slow diffusion of Et_2O into a saturated THF solution of **2a**. Yellow plates of [Ru(H$_2$)(PCy$_3$)('N$_2$Me$_2$S$_2$')]·0.5 pentane (**2b**·0.5 pentane) formed over two weeks at 10 °C on slow diffusion of *n*-pentane into a saturated THF solution of **2b**. Yellow blocks of [Ru(BH$_3$)(P*i*Pr$_3$)('N$_2$Me$_2$S$_2$')] (**3a**) were grown at room temperature over two weeks by slow diffusion of Et_2O into a saturated THF solution of **3a**. Yellow blocks of [Li(thf)$_2$][Ru(H)(P*i*Pr$_3$)('N$_2$Me$_2$S$_2$')] [Li(thf)$_2$]-**4a**) were obtained over two months at −34 °C by layering a saturated THF solution of **3a** with *n*-pentane. Red needles of NBu_4[Ru(H)(PCy$_3$)('N$_2$Me$_2$S$_2$')]·0.83 Et_2O·0.17 THF (NBu_4**4b**·0.83 Et_2O·0.17 THF) were obtained over three weeks at 20 °C by slow diffusion of Et_2O into a saturated THF solution of **1b**. Intensity data were collected at 100 K on a Bruker-Nonius Kappa CCD diffractometer using $Mo_{K\alpha}$ radiation ($\lambda = 0.71073$ Å, graphite monochromator) and corrected for Lorentzian and polarization effects. Absorption effects were taken into account by using multiscan procedures (**2a**, NBu_4**4b**·83 Et_2O·0.17 THF: SORTAV;[29] **2b**·0.5 pentane, [Li(thf)$_2$]-**4a**: SADABS[30]) or applying a numerical correction (**3a**).[31] All structures were solved by direct methods and refined by full-matrix least-squares procedures (**2b**, **3b**, **3c**: SHELXTL NT 6.12;[32] **2a**, **4a**: SHELXTL NT 5.10[33]). The Li ion in **3a** is coordinated by two THF molecules. With the exception of NBu_4**4b**·0.83 Et_2O·0.17 THF, for which only the hydride H atom position was taken from a difference Fourier map, the positions of all H atoms were localized in difference Fourier syntheses. These hydrogen atoms were refined with a fixed common isotropic displacement parameter (**2a**, **3a**, [Li(thf)$_2$]-**4a**) or were not refined (**2b**·0.5 pentane). Hydrogen atoms of NBu_4**4b**·0.83 Et_2O·0.17 THF were geometrically positioned. The molecule of solvation in **2b**·0.5 pentane is disordered on a crystallographic inversion center, and no H atoms were included for this. The Et_2O of solvation in NBu_4**4b**·0.83 Et_2O·0.17 THF is located on two crystallographic sites, the second of which is shared with a THF molecule in a ratio of 0.33:0.17. Selected crystallographic data for complexes **2** to **4** are summarized in Table 2.

CCDC-229678 (**2a**), CCDC-229679 (**2b**), CCDC-229680 (**3a**), CCDC-229681 (**4a**), and CCDC-229682 (**4b**) contain the supplementary crystallographic data for this paper. These data can be obtained free of charge via www.ccdc.cam.ac.uk/conts/retrieving.html (or from the Cambridge Crystallographic Data Centre, 12 Union Road, Cambridge CB2 1EZ, UK; fax: (+44) 1223-336-033; or deposit@ccdc.cam.uk).

DFT calculations: For all calculations we used the density functional programs provided by the TURBOMOLE 5.1 suite.[35] All results were obtained from all-electron Kohn–Sham calculations. We employed the Becke–Perdew functional dubbed BP86[36,37] and the hybrid functional B3LYP[38,39] as implemented in TURBOMOLE. In connection with the BP86 functional we always used the resolution of identity (RI) technique.[40,41] These two functionals were chosen since they are the best established representatives of pure and hybrid density functionals and yield reasonable reaction energetics in a large number of cases. However, the situation is different for iron compounds, for which highly unreliable energetics were obtained for complexes of the type under study.[42] A systematic study has shown that transition metal complexes in general may represent critical cases when high-spin/low-spin energy splittings are small, and results can differ greatly when calculated with pure and hybrid density functionals.[43] To test internal consistency we used in addition to BP86 and B3LYP our reparametrized B3LYP, dubbed B3LYP*, which was developed especially for these complexes[43] but which is of general applicability.[44] The influence of the size of the basis set was studied for similar mononuclear iron complexes of the compound under study[45] by means of three different basis sets. The first, denoted SV(P), is the split-valence basis set[46] with polarization functions on heavy atoms, but not on hydrogen atoms. Moreover, we used the TZVP basis set of Ahlrichs et al.,[47] which features a valence triple-zeta basis set with polarization

Table 2. Selected crystallographic data of **2a**, **2b**·0.5 pentane, **3a**, [Li(thf)$_2$]-**4a**, and NBu_4-**4b**·0.83 Et_2O·0.17 THF.

Complex	**2a**	**2b**	**3a**	**4a**	**4**
formula	$C_{25}H_{41}N_2PRuS_2$	$C_{36.5}H_{59}N_2PRuS_2$	$C_{25}H_{42}BN_2PRuS_2$	$C_{33}H_{56}LiN_2O_2PRuS_2$	$C_{54}H_{97.66}N_3OPRuS_2$
M_r	565.76	722.02	577.58	715.90	1001.17
crystal size [mm]	0.32 × 0.22 × 0.10	0.25 × 0.17 × 0.05	0.36 × 0.24 × 0.16	0.42 × 0.20 × 0.12	0.25 × 0.18 × 0.14
F(000)	1184	1532	2416	756	2167
space group	$P2_1/c$	$P2_1/c$	$Pbca$	$P\bar{1}$	$Pca2_1$
crystal system	monoclinic	monoclinic	orthorhombic	triclinic	orthorhombic
a [pm]	1506.99(9)	1744.0(2)	1335.0(2)	1023.9(1)	3308.1(3)
b [pm]	1178.84(9)	1188.3(1)	1593.0(2)	1264.64(4)	1094.79(9)
c [pm]	1431.86(3)	1813.8(2)	2541.4(2)	1518.77(8)	1572.68(7)
α [°]	90	90	90	111.596(5)	90
β [°]	91.024(4)	112.341(6)	90	105.859(7)	90
γ [°]	90	90	90	92.120(5)	90
V [nm^3]	2.5433(3)	3.4768(6)	5.4047(9)	1.7379(2)	5.6957(7)
Z	4	4	8	2	4
ρ_{calcd} [g cm^{-3}]	1.478	1.379	1.420	1.368	1.168
μ [mm^{-1}]	0.860	0.645	0.810	0.648	0.413
2θ range [°]	6.3–60.0	6.5–54.2	6.0–56.0	6.0–58.0	5.2–52.0
T_{min}; T_{max}	0.677; 0.923	0.868; 1.000	0.789; 0.894	0.758; 1.000	0.914; 0.949
meas. reflns.	60483	33467	32666	42000	35559
indep. reflns.	7409	7644	6464	9204	10479
R_{int}	0.0794	0.1442	0.0889	0.0777	0.0697
obsd. reflns.	5825	4771	4612	6713	8243
R_1; wR_2 (all data)	0.0339; 0.0691	0.0543; 0.1131	0.0450; 0.0988	0.0432; 0.1009	0.0571;0.1558
ref. par.	405	388	415	499	634
$\Delta\delta_{max/min}$	0.514/−0.731	0.884/−0.793	0.726/−1.618	0.670/−0.710	0.581/−0.772
abs. struct. par.[34]	–	–	–	–	0.04(4)

functions on all atoms. For a sufficiently large number of test calculations on iron(II) analogues the TZVP and TZVPP reaction energies differed by only about 5 kJ mol^{-1} without correcting for the basis-set superposition error (BSSE).[45] If a counterpoise correction is added, our test calculations on coordination energies have shown that results obtained with the TZVP and the TZVPP basis set differ by less than about 1 kJ mol^{-1}. For reasons of computational efficiency, we used the TZVP basis set and a simplified model of the experimental complexes, in which we replaced the phosphane by PH_3 and the methyl groups at the nitrogen atoms of the chelate ligand by hydrogen atoms. All structures were optimized with the corresponding density functional and basis set.

Table 3 lists the coordination energies for the coordination of N_2 and H_2 to the (relaxed) five-coordinate metal fragment (these energies were neither corrected for the zero-point vibrational energy nor for the basis set superposition error, but a counterpoise correction[48,49] would lower the absolute value of the coordination energy by less than 5 kJ mol^{-1}, as test calculations on this type of complexes have shown (BP86/RI/TZVP).

Table 3. Coordination energies [kJ mol^{-1}] of N_2 and H_2 to [Ru(PR$_3$)('N$_2$Me$_2$S$_2$')] fragments (R = *i*Pr, Cy).

	BP86/RI/TZVP	B3LYP/TZVP	B3LYP*/TZVP
N_2	−95.5	−87.0	−93.7
H_2	−87.5	−75.4	−78.5
CED[a]	8.0	11.5	15.2

[a] Coordination-energy difference for N_2 and H_2.

Acknowledgement

Help from Prof. Dr. H. Kisch and Dr. J. Sutter, Institut für Anorganische Chemie der Universität Erlangen-Nürnberg, and from Prof. Dr. H. Zimmermann, Institut für Angewandte Physik der Universität Erlangen-Nuremberg is gratefully acknowledged. We thank the Deutsche Forschungsgemeinschaft (SFB 583) and the Fonds der Chemischen Industrie for financial support.

[1] a) E. K. Jackson, G. W. Parshall, R. W. F. Hardy, *J. Biol. Chem.* **1968**, *243*, 4952–4958; b) R. W. F. Hardy, R. D. Holsten, E. K. Jackson, R. C. Burns, *Plant Physiol.* **1968**, *43*, 1185–1207.
[2] B. K. Burgess, D. J. Low, *Chem. Rev.* **1996**, *96*, ,2983–3011.
[3] a) R. N. F. Thornely, D. J. Lowe, *J. Biol. Inorg. Chem.* **1996**, *1*, 576–580; b) I. G. Dance, *J. Biol. Inorg. Chem.* **1996**, *1*, 581–586; c) D. Sellmann, J. Sutter, *J. Biol. Inorg. Chem.* **1996**, *1*, 587–593; d) D. Coucouvanis, *J. Biol. Inorg. Chem.* **1996**, *1*, 594–600; e) C. J. Pickett, *J. Biol. Inorg. Chem.* **1996**, *1*, 601–606.
[4] D. V. Yandulov, R. R. Schrock, *J. Am. Chem. Soc.* **2002**, *124*, 6252–6253, and references therein.
[5] M. D. Fryzuk, B. A. MacKay, B. O. Patrick, *J. Am. Chem. Soc.* **2003**, *125*, 3234–3235.
[6] a) R. N. F. Thornely, D. J. Lowe, J. David, *Met. Ions Biol.* **1985**, *7 (Molybdenum Enzymes)*, 221–284; b) B. E. Smith, P. E. Bishop, R. A. Dixon, R. R. Eady, W. A. Filler, D. J. Lowe, A. J. M. Richards, A. J. Thomson, R. N. F. Thornely, J. R. Postgate, *Nitrogen Fixation Res. Prog. Proc. Int. Symp. 6th* **1985**, 597–603; c) D. L. Hughes, S. K. Ibrahim, C. J. Pickett, G. Querne, A. Lauoenan, J. Talarmin, A. Queiros, A. Fonseca, *Polyhedron* **1994**, *13*, 3341–3348; d) G. N. Schrauzer, J. G. Palmer, *Z. Naturforsch. B* **2001**, *56*, 386–393; G. N. Schrauzer, *Angew. Chem.* **1975**, *87*, 579–87; *Angew. Chem. Int. Ed. Engl.* **1975**, *14*, 514–522.
[7] D. Sellmann, A. Fürsattel, A. Sutter, *J. Coord. Chem.* **2000**, *545*, 200–202.
[8] R. A. Henderson, *Recent Advances in Hydride Chemistry*, Elsevier Science, Amsterdam **2001**, pp. 463–505.
[9] D. Sellmann, B. Hautsch, A. Rösler, F. W. Heinemann, *Angew. Chem.* **2001**, *113*, 1553–1558; *Angew. Chem. Int. Ed.* **2001**, *40*, 1505–1507.
[10] D. Sellmann, A. Hille, F. W. Heinemann, M. Moll, A. Rösler, J. Sutter, G. Brehm, M. Reiher, B. A. Hess, S. Schneider, *Inorg. Chim. Acta* **2003**, *348*, 194–198.
[11] G. J. Kubas, *Metal Dihydrogen and σ-Bond Complexes*, Kluwer Academic/Plenum, New York, **2001**, pp. 46–47.
[12] D. Sellmann, T. Gottschalk-Gaudig, F. W. Heinemann, *Inorg. Chem.* **1988**, *37*, 3982–3988.
[13] D. Sellmann, R. Prakash, F. W. Heinemann, M. Moll, M. Klimowicz, *Angew. Chem.* **2004**, *116*, 1913; *Angew. Chem. Int. Ed.* **2004**, *43*, 1877–1880.
[14] a) [Fe(BH$_3$)(CO)(PPh$_3$)$_2$(methyldithioformate)]: D. V. Khasnis, L. Toupet, P. H. Dixneuf, *Chem. Commun.* **1987**, 230–231; b) [Ru(BH$_3$)(H)(1,1,1-tris(diphenylphosphanymethyl)ethane)(2-ethylthiophenol)]: C. Bianchini, D. Masi, A. Mell, M. Peruzzini, F. Vizza, F. Zanobini, *Organometallics* **1998**, *17*, 2495–2502.
[15] J. A. Ayollon, C. Gerveaux, S. Sabo-Etienne, B. Chaudret, *Organometallics* **1997**, *16*, 2000–2002.
[16] *Transition Metal Hydrides* (Ed.: E. L. Muetterties), Marcel Dekker, New York, **1971**.
[17] a) P. G. Jessop, R. H. Morris, *Coord. Chem. Rev.* **1992**, *121*, 155–284; b) D. M. Heinekey, W. J. Oldham, *Chem. Rev.* **1993**, *93*, 913–926; c) P. J. Desrosiers, L. Cai, Z. Lin, R. Richards, J. Halpern, *J. Am. Chem. Soc.* **1991**, *113*, 4173–4184.
[18] a) M. S. Chinn, D. M. Heinekey, *J. Am. Chem. Soc.* **1987**, *109*, 5865–5867; b) P. A. Maltby, M. Schlaf, M. Steinbeck, A. J. Lough, R. H. Morris, W. T. Klooster, T. F. Koetzle, R. C. Srivastava, *J. Am. Chem. Soc.* **1996**, *118*, 5396–5407; c) J. K. Law, H. Mellows, D. M. Heinekey, *J. Am. Chem. Soc.* **2002**, *124*, 1024–1030.
[19] B. D. Nageswara Rao, L. R. Anders, *Phys. Rev. A* **1965**, *140*, 112–117.
[20] G. J. Kubas, *Comments Inorg. Chem.* **1988**, *7*, 17–40.
[21] a) M. T. Bautista, E. P. Cappellani, S. D. Drouin, R. H. Morris, C. T. Schweitzer, A. Sella, J. J. Zubkowski, *J. Am. Chem. Soc.* **1991**, *113*, 4876–4887; b) M. T. Bautista, K. A. Earl, P. A. Maltby, R. H. Morris, C. T. Schweitzer, A. Sella, *J. Am. Chem. Soc.* **1988**, *110*, 7031–7036.
[22] D. Sellmann, H. G. Rackelmann, F. W. Heinemann, *Eur. J. Chem.* **1987**, 2071–2080.
[23] D. Sellmann, A. Hille, A. Rösler, M. Moll, F. W. Heinemann, *Inorg. Chim. Acta*, **2004**, in press.
[24] D. Sellmann, A. Hille, M. Moll, W. Bauer, F. W. Heinemann, B. A. Hess, M. Reiher, A. Rösler, *Chem. Eur. J.* **2004**, *10*, 819–830.
[25] R. H. Morris, K. A. Earl, R. L. Luck, N. J. Lazarowych, A. Sella, *Inorg. Chem.* **1987**, *26*, 2674–2683.
[26] S. J. Lippard, K. M. Melmed, *J. Am. Chem. Soc.* **1967**, *89*, 3929–3930.
[27] H. Noth, R. Hartwimmer, *Chem. Ber.* **1960**, *93*, 2238–2245.
[28] P. H. Bird, M. R. Churchill, *J. Chem. Soc. Chem. Commun.* **1967**, 403.
[29] R. H. Blessing, *Acta Crystallogr. Sect. A* **1995**, *52*, 33–38.
[30] Bruker-AXS **2002**, Madison, WI, USA.
[31] P. Coppens in *Crystallographic Computing* (Eds.: F. R. Ahmed, S. R. Hall, C. P. Huber), Munksgaard, Copenhagen, **1970**, pp. 255–270.
[32] SHELXTL NT 6.12, Bruker-AXS **2002**, Madison, WI, USA.
[33] SHELXTL NT 5.10, Bruker-AXS **1998**, Madison, WI, USA.
[34] H. D. Flack, *Acta Crystallogr. Sect. A* **1983**, *39*, 876–881.
[35] R. Ahlrichs, M. Bär, M. Häser, H. Horn, C. Kölmel, *Chem. Phys. Lett.* **1989**, *162*, 165–169.
[36] A. D. Becke, *Phys. Rev. A* **1988**, *38*, 3098–3100.
[37] J. Perdew, *Phys. Rev. B* **1986**, *33*, 8822–8824.
[38] A. D. Becke, *J. Chem. Phys.* **1993**, *98*, 5648–5652.
[39] P. J. Stephens, F. J. Devlin, C. F. Chabalawski, M. J. Frisch, *J. Phys. Chem.* **1994**, *98*, 11623–11627.
[40] K. Eichkorn, O. Treutler, H. Öhm, M. Häser, R. Ahlrichs, *Chem. Phys. Lett.* **1995**, *240*, 283–290.
[41] K. Eichkorn, F. Weigend, O. Treutler, R. Ahlrichs, *Theor. Chem. Acc.* **1997**, *97*, 119–124.
[42] M. Reiher, O. Salomon, D. Sellmann, B. A. Hess, *Chem. Eur. J.* **2001**, *7*, 5195–5202.
[43] M. Reiher, O. Salomon, B. A. Hess, *Theor. Chem. Acc.* **2001**, *107*, 45–55.

[44] O. Salomon, M. Reiher, B. A. Hess, *J. Chem. Phys.* **2002**, *117*, 4729–4737.
[45] M. Reiher, B. A. Hess, *Chem. Eur. J.* **2002**, *8*, 5332–5339.
[46] A. Schäfer, H. Horn, R. Ahlrichs, *J. Chem. Phys.* **1992**, *97*, 2571–2577.
[47] A. Schäfer, C. Huber, R. Ahlrichs, *J. Chem. Phys.* **1994**, *100*, 5829–5835.
[48] S. F. Boys, F. Bernardi, *Mol. Phys.* **1970**, *19*, 553–566.
[49] F. B. van Duijnevetdt, J. G. C. M. van Duijenveld-van de Rijdt, J. H. van Lente, *Chem. Rev.* **1994**, *94*, 1873–1885.

Received: February 5, 2004
Published online: July 14, 2004

